Dielectric studies of glass transition in confined propylene glycol

1998 J. Phys.: Condens. Matter 10 6205

(http://iopscience.iop.org/0953-8984/10/28/004)

J. Phys.: Condens. Matter **10** (1998) 6205–6227. Printed in the UK PII: S0953-8984(98)88495-6

Dielectric studies of glass transition in confined propylene glycol

P Pissis†, A Kyritsis†, D Daoukaki†, G Barut‡, R Pelster‡ and G Nimtz‡

† National Technical University of Athens, Department of Physics, Zografou Campus, GR-15773 Athens, Greece

‡ Universität zu Köln, II Physikalisches Institut, Züplicher strasse 77, 50937 Cologne, Germany

Received 16 October 1997, in final form 15 April 1998

Abstract. The dynamical behaviour of the glass transition of propylene glycol confined in droplets in butyl rubber (three-dimensional confinement, mean droplet diameter $d = 8$–11 nm) and in pores in controlled porous glasses (two-dimensional confinement, mean pore diameter $d = 2.5$–7.5 nm) has been studied in detail by means of broadband dielectric spectroscopy (5 Hz–2 GHz) and of thermally stimulated depolarization current measurements. Effective medium theory corrections of the data are discussed. The results indicate the existence of a relatively immobile interfacial layer close to the wall. For the volume liquid the dynamics of the glass transition becomes faster and the glass transition temperature T_g decreases compared to the bulk liquid. The shifts ΔT_g increase with decreasing d, are larger in butyl rubber than in controlled porous glasses (three-dimensional versus two-dimensional confinement) and vanish for $d \approx 10$–12 nm. These results are discussed in relation to those obtained with polymers confined in thin polymeric films (one-dimensional confinement) and in semicrystalline polymeric samples and are explained on the basis of the cooperativity concept and the model of Adam and Gibbs. The cooperativity length ξ at T_g is determined to be $\xi \leqslant 5$–6 nm in both butyl rubber and controlled porous glasses. Interesting effects of confinement are observed on the shape of the dielectric response of the process associated with the glass transition.

1. Introduction

The glass transition, that is the freezing of a supercooled liquid into an amorphous solid, is a central problem of condensed-matter physics [1–3]. There exist several theoretical approaches to but no generally accepted theory of it. The investigation of effects on glass transition induced by confinement of glass-forming liquids and of amorphous polymers in mesoscopic volumes may provide additional information on the dynamics of glass transition and may help to check theories and models proposed for it [4–8]. This expectation is based on the central role of the cooperativity concept in many theories and models for the glass transition (however not in the very popular mode coupling theory [2]).

The plausible idea of molecules rearranging themselves cooperatively within regions of a characteristic size in an undercooled liquid near the glass transition has been made quantitative in the configurational entropy model of glass formation of Adam and Gibbs [9]. According to this model, developed for a bulk system, the molecules whose motions are correlated form a cluster and the system comprises a number of such clusters, called 'cooperatively rearranging regions'. The size of the cluster (sphere of radius ξ) is related to its content of configurational entropy [9]. ξ, the cooperativity length or characteristic length of glass transition, increases with decreasing temperature until, at a certain temperature,

0953-8984/98/286205+23$19.50

the cooperative region comprises the whole system causing the sharp reduction of mobility observed in the experiments. The existence of size effects on glass transition is a direct consequence of the cooperativity concept [4, 8]. If the size of the sample confined in a small volume is less than ξ, deviations from the bulk dynamic behaviour should be observed. These deviations should decrease with increasing sample size and disappear for samples larger than ξ. Moreover, the experimental observation of size effects would yield ξ most directly [4]. In real experiments with confined glass-forming liquids and polymers the interaction of molecules or chains with the walls or the substrate (chemical effects) may mask the pure confinement (physical) effects [4, 10–13].

Differential scanning calorimetry (DSC) measurements on several glass-forming liquids confined in the pores of controlled porous glasses (CPGs) of diameters in the range of nm show a decrease of the glass transition temperature T_g and a broadening of the glass transition region [14, 15]. These effects have been assigned to reduction of the density of the liquid in the pores [14] and to capillary effects [15]. On the other hand, DSC measurements on liquids confined in microemulsions [16] and in hydrogels [17] show a significant broadening of the glass transition but practically no shift of T_g compared to bulk liquids.

In a previous paper [6] we used, for the first time, dielectric relaxation spectroscopy (DRS) and thermally stimulated depolarization current (TSDC) measurements to study size effects on the glass transition dynamics in three glass-forming liquids, glycerol, propylene glycol and propylene carbonate, confined in the 4.0 nm pores of Vycor glass. Confinement was found to induce an acceleration of the α relaxation associated with the glass transition and a shift of T_g to lower temperatures, as well as a broadening of the relaxation and a change of its shape. DRS and solvation dynamics measurements by other investigators on several glass-forming liquids confined in different CPGs with pore diameters between 2.5 and 10.2 nm show, in addition to commonly observed broadening of the α relaxation, small shifts to both higher and lower temperatures, depending on liquid and CPG [18–22].

Common to all CPGs used for confinement studies so far is that the liquid is confined in pores, i.e. confinement is two dimensional (2D). In this work we extend our studies on size effects on the glass transition dynamics by means of DRS and TSDC measurements to include, for the first time, confinement of liquids in butyl rubber (BR) containing hydrophilic inclusions, where the liquid is confined in droplets, i.e. in three dimensions [23]. It should be noted that also in liquids confined in microemulsions and studied by DSC [16] confinement was three dimensional (3D). Our methodology is somewhat different than in most previous relevant investigations. We restrict our study to one liquid only, propylene glycol (PG) as a representative of hydrogen bonded liquids, confined in three different systems: in BR (3D confinement, in the form of droplets with diameters in the range 8–11 nm) and in two CPG systems (2D confinement), Vycor glass with pore diameter 4.0 nm and sol–gel glasses with pore diameters 2.5, 5.0 and 7.5 nm. The use of several confining systems with different dimensionality and confining length may also allow us to distinguish between pure confinement and surface effects [4, 10–13].

The techniques used include broadband DRS and TSDC. DRS (5 Hz–2 GHz, 170–300 K) allows us to follow the overall dielectric behaviour, and the dynamics of the α relaxation in particular, in wide ranges of frequency and temperature. TSDC techniques, characterized by high sensitivity and high resolving power [24], allow us to record the dielectric response of the sample as a function of temperature (77–300 K) at cooling and heating rates comparable to those used in DSC. Information on size effects on the dynamic glass transition is then obtained from the overall dielectric response and from the properties of the α relaxation (temperature dependence of relaxation rate, shift of glass transition

temperature T_g and shape of the response). Maxwell–Garnett theory is employed to regain the dielectric behaviour of the confined liquid from that of the composite BR–PG system [25–27].

The results obtained here with PG in 2D and in 3D confinement will be discussed in relation to those obtained with thin polymeric films (one-dimensional, 1D confinement) [11, 13, 28–32], with amorphous polymers confined in semicrystalline polymers [33, 34] and with confined liquid crystals [8, 35, 36] and in terms of theories and models of the glass transition.

2. Materials and methods

2.1. Materials

Propylene glycol (99.9%) was obtained from Sigma, St Louis and used without further treatment.

Butyl rubber (BR) with hydrophilic components was provided by Bayer, AG, Leverkusen. Similar samples have been used in a previous investigation on the properties of mesoscopic water droplets dispersed in BR [23]. We refer to that paper for details concerning the BR samples. To fill BR samples with PG, dry samples (circular sheets of 15 mm diameter and 1 mm thickness) were placed in a PG bath in an autoclave (443 K, 2.3 bar). The weight of the BR samples was recorded as a function of time and it was found that diffusion followed Fickian behaviour. By this procedure samples with several filling factors f, defined as liquid volume in the sample divided by sample volume, between 7.1 and 16.4% were prepared. f remains practically constant over longer periods when samples thus prepared are kept immersed in PG at room temperature. For details of sample preparation we refer to [37]. Small angle x-ray scattering (SAXS) measurements on the PG filled BR samples showed that, similar to water in BR [23], PG is organized in droplets with droplet diameters d in the range 8–11 nm increasing approximately linearly with increasing filling factor f [37]. The distribution of droplet diameters is characterized by relative half widths (half width divided by the diameter of maximum in the distribution of droplet diameters) of about 0.3 [37].

Vycor glass samples (Corning, No 7930) with porosity (pore volume) 28%, internal surface area 250 $m^2\ g^{-1}$ and an average pore diameter of 4.0 nm, were of cylindrical shape with 15 mm diameter and about 1 mm thickness. They were cleaned and dried according to the producer's instructions and filled to saturation by immersion in PG.

Gelsil glass samples, produced by sol–gel technology, purchased from GelTech Inc., USA, were of cylindrical shape with 10 mm diameter and about 1 mm thickness. The nominal pore diameters are 2.5, 5.0 and 7.5 nm, the porosities 48, 63 and 70% and the internal surface areas 610, 580 and 525 $m^2\ g^{-1}$. Samples were cleaned and dried according to the producer's instructions and filled to saturation by immersion in PG.

2.2. Methods of measurements

For broadband DRS measurements 5 Hz–2 GHz, 170–300 K, the BR and the CPG samples were placed in a shielded capacitor-like measurement cell with nickel-coated stainless steel electrodes in a homemade thermostatic oven and the transmission coefficients of the experimental set-up were measured (network analysers HP 3577B and HP 8510B from 5 Hz to 200 MHz and 200 MHz to 2 GHz, respectively). A novel calibration method allows accurate evaluation in the whole frequency range with the same sample geometry in

a single sweep [38]. The temperature was controlled to better than 0.1 K measured over the period of a frequency sweep. For the measurements on bulk PG the cell consists of two nickel-coated stainless steel electrodes (with a diameter of 15 mm) separated by 50 μm thick silica spacers. For details of measurements we refer to [37].

TSDC measurements, which correspond to measurements of dielectric losses against temperature at fixed frequencies of 10^{-2}–10^{-4} Hz [24], were carried out in the temperature range 77–300 K on the same samples as used for DRS measurements. The BR and the CPG samples were clamped between brass electrodes. A disc sample geometry was used also for measurements on bulk PG with brass electrodes of 8 mm diameter. The method has been described in detail elsewhere [24, 39]. Here we recall briefly the TSDC procedure. The sample is polarized by a dc electric field E_p at temperature T_p for a time t_p and its polarization is quenched at a sufficiently low temperature T_0. By warming the sample at a linear heating rate b in short-circuit conditions, the polarization decays and the corresponding depolarization current is detected by an electrometer. For each relaxation mechanism an inherent current peak is recorded. The analysis of the shape of the recorded thermogram allows us to obtain the contribution $\Delta\varepsilon$ of a peak to the static permittivity and the thermodynamic and form parameters of the underlying relaxation mechanism [24, 39]. For details of the apparatus used we refer to [39].

3. Experimental results

3.1. The overall dielectric response

Figure 1 shows in log–log plots the overall behaviour of dielectric loss ε'' against frequency ν at several selected temperatures for PG bulk (a) and PG confined in Gelsil glasses with mean pore diameter $d = 2.5$ nm (b) and in BR with filling factor $f = 16.4\%$ and mean droplet diameter $d = 10.2$ nm (c). For bulk PG we observe a loss peak at high frequencies due to the main (primary) a relaxation associated with the glass transition ($T_g = 167$ K). At low frequencies ε'' increases with decreasing frequency with a slope of -1 due to dc conductivity σ_{dc},

$$\varepsilon''(\nu) = \sigma_{dc}/\varepsilon_0\omega \tag{1}$$

where ε_0 is the permittivity of free space and $\omega = 2\pi\nu$ [40]. For confined PG we observe, in addition to the α process, a broad complex dispersion region at lower frequencies and a conductivity wing for Gelsil (however, not for BR).

In figure 2 we compare with each other the overall dielectric behaviour of PG bulk and PG confined in BR ($f = 16.4$, $d = 10.2$ nm) at 253 K. In order to analyse the complex response of PG confined in BR the following strategy was adopted. The two-shape-parameter Havriliak–Negami (HN) expression [40]

$$\varepsilon^*(\nu) = \varepsilon_\infty + \frac{\Delta\varepsilon}{[1 + (\mathrm{i}\nu/\nu_{HN})^{1-\alpha}]^\gamma} \tag{2}$$

was fitted to the α process (for bulk liquid too). In this expression $\varepsilon^* = \varepsilon' - \mathrm{i}\varepsilon''$ is the complex dielectric function (permittivity), $\Delta\varepsilon$ and ν_{HN} are, respectively, the intensity (strength) and the position on the frequency scale of the relaxation process, ε_∞ is $\varepsilon'(\nu)$ for $\nu \gg \nu_{HN}$ and α and γ are the shape parameters. The broad complex dispersion region was fitted by a sum of two (the lowest possible) relaxations, Rel I and Rel II in the order of increasing frequency, each of them described by the one-shape-parameter symmetric

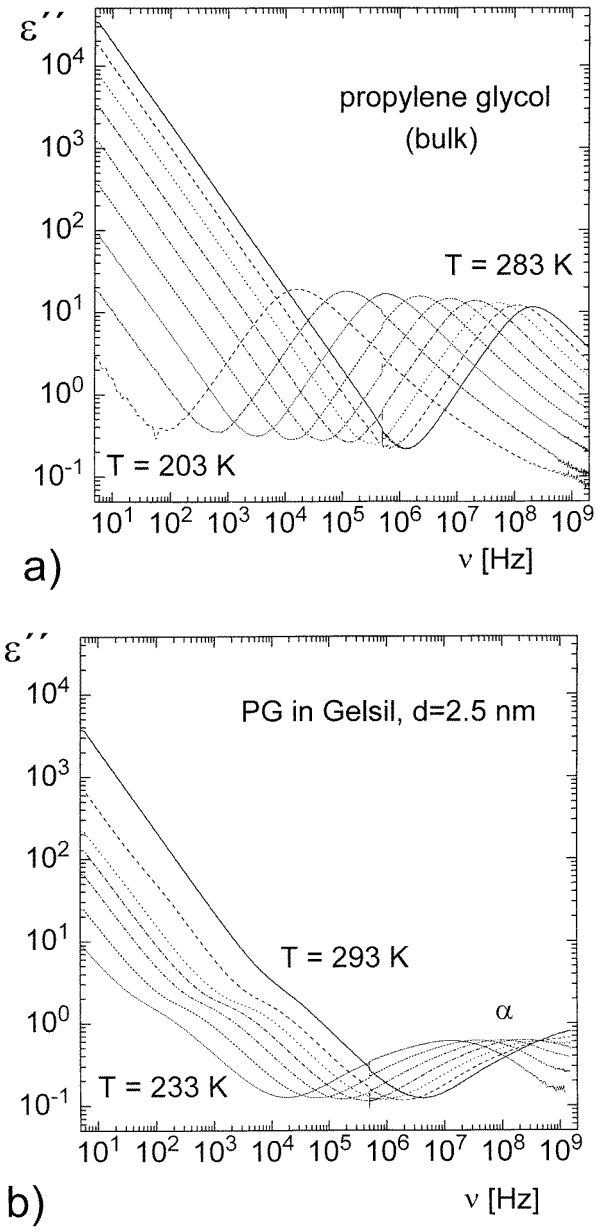

Figure 1. Log–log frequency plots of dielectric loss $\varepsilon''(\nu)$ at several selected temperatures for PG bulk (a), PG confined in Gelsil glasses with mean pore diameter $d = 2.5$ nm (b) and PG confined in BR with filling factor $f = 16.4\%$ and mean droplet diameter $d = 10.2$ nm (c).

Cole–Cole (CC) expression [40]

$$\varepsilon^*(\nu) = \varepsilon_\infty + \frac{\Delta\varepsilon}{1 + (\mathrm{i}\nu/\nu_{cc})^{1-\alpha}} \tag{3}$$

i.e. with $\gamma = 1$ in (2). The HN and the CC fits were satisfactory and the values of fit parameters meaningful at each temperature and filling factor.

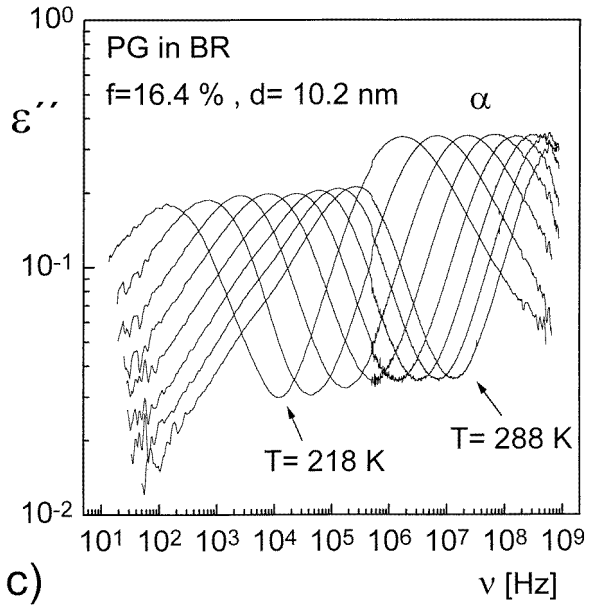

Figure 1. (Continued)

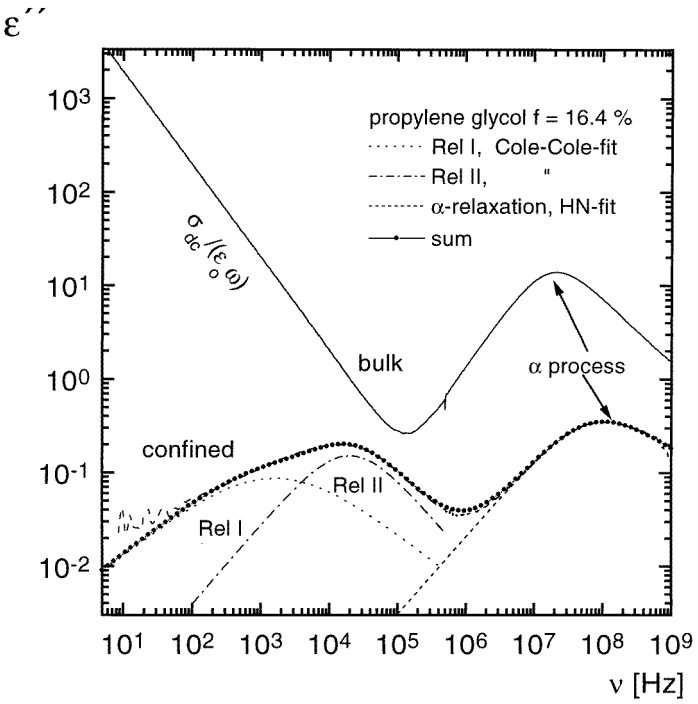

Figure 2. Log–log frequency plots of dielectric loss $\varepsilon''(\nu)$ for PG bulk and confined in BR (filling factor $f = 16.4\%$, mean droplet diameter $d = 10.2$ nm) at 253 K, details in text.

As indicated in figure 1, the main difference of $\varepsilon''(\nu)$ plots measured on PG confined in CPG, compared to those measured on PG confined in BR, is that conductivity effects

dominate at low frequencies, in agreement with previous investigations [6, 18–21]. To account for that a power law term [41],

$$\varepsilon^*(\nu) = -\mathrm{i}\sigma_{dc}/\varepsilon_0(2\pi\nu)^s \tag{4}$$

with $s \leqslant 1$ ($s = 1$ for ohmic conductivity) is added to the sum of the CC terms representing Rel I and Rel II, with the result that the analysis becomes less unambiguous for CPG compared to BR.

Rel I and Rel II are assigned to a slow liquid surface layer and to interfacial Maxwell–Wagner–Sillars polarization, respectively, in agreement with the results of detailed Maxwell–Wagner–Sillars calculations for heterogeneous systems. The calculations allow us to predict both the dielectric relaxation time and the dielectric strength of the interfacial Maxwell–Wagner–Sillars relaxation, which are in good agreement with the experimental data for Rel II. For details we refer to [37]. Additional support for this interpretation comes from the results of a similar analysis for N-methyl-ε-caprolactam in CPG [19] and from measurements on chemically modified and on partially filled CPG systems [19]. In what follows we focus on the α process.

The dielectric data for the α process in figures 1 and 2 are effective values [26, 27]. They refer to the composite material consisting of the glass or polymer matrix and the liquid inclusions. Effective medium theories can be used to calculate the dielectric data for the confined liquid from the data measured on the composite material [25]. This procedure is straightforward in the case of BR where the liquid is confined in spherical droplets, as indicated by the SAXS experiments [37]. Here we used the Maxwell–Garnett theory [26, 27] to calculate the relaxation rates and the dielectric strength of the α process for PG confined in BR from the corresponding measured effective data.

The Maxwell–Garnett formula is [26, 27]

$$\varepsilon_{eff} = \varepsilon_m\left(1 + \frac{1}{D}\frac{fx}{1-fx}\right) \qquad \text{for } f|x| \ll 1 \tag{5}$$

where

$$x = \frac{D(\varepsilon_p - \varepsilon_m)}{\varepsilon_m + D(\varepsilon_p - \varepsilon_m)}. \tag{6}$$

In these equations ε_{eff}, ε_m and ε_p are the complex dielectric function of the composite material, the matrix and the inclusion, respectively. The depolarization factor D depends on the form of the inclusions; $D = 1/3$ for spherical inclusions. f is the volume filling factor.

3.2. Arrhenius plots

Figure 3 shows the Arrhenius plot for the α process of PG bulk and of PG confined in Vycor glass (mean pore diameter $d = 4.0$ nm). Similar plots are shown in figure 4(a) for PG in BR at different filling factors and droplet diameters. The measured effective values in figure 4(a) were corrected using the Maxwell–Garnett formula (5) and reasonable approximations. The calculations (details to be published elsewhere) show that the corrected relaxation rates are smaller than the measured effective ones by a factor of about five to nine depending on filling factor and temperature. The corrected relaxation rates for the f and d values of figure 4(a) are shown in figure 4(b). We observe that, in general, the relaxation becomes faster in the confined liquid: for the same temperature the loss peak shifts to higher frequencies (compare also figure 2) and for the same frequency (isochronal plot) the loss peak shifts to lower temperatures. In figure 4 we observe that the shifts compared

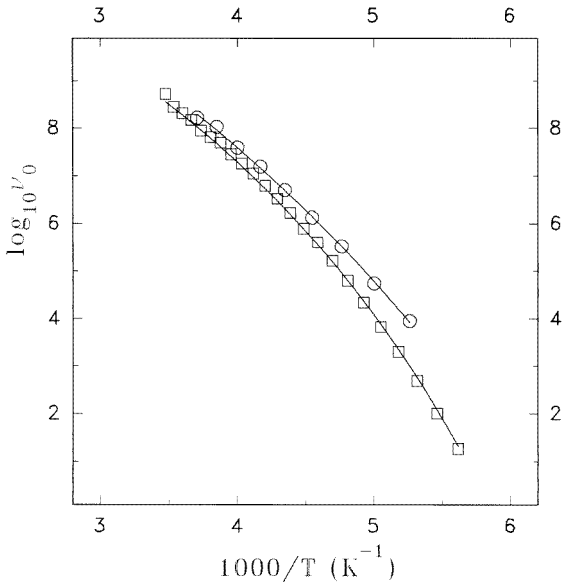

Figure 3. Arrhenius plot (semilogarithmic plot of frequency of maximum dielectric loss, ν_0, against reciprocal temperature, $1/T$) for the α process in PG bulk (□) and PG confined in Vycor glass (○, mean pore diameter $d = 4.0$ nm). The lines are VFT (7) fits to the data.

to the bulk response, increase with decreasing droplet diameter. Similar behaviour is also observed with PG in Gelsil glasses. An additional feature in figures 3 and 4 is that the shifts decrease with increasing temperature/increasing frequency, i.e. confinement effects become less pronounced with increasing temperature and finally disappear (figure 4(b)). Comparison of figures 4(a) and 4(b) with each other suggests that the acceleration of the α process for the confined liquid as measured by DRS is partly due to the conditions of measurement (effective medium) and partly due to confinement effects [25]. Moreover, the corrected relaxation rates become equal to the bulk ones at sufficiently high temperatures (for PG in BR with $d = 8$–11 nm at $T \geqslant T_g + 50$ K). The corrections are expected to be less significant in the case of CPG, because of both the shape of inclusions (interconnected pores) and the higher filling factors.

The Vogel–Fulcher–Tammann (VFT) expression [1–3]

$$\nu_0 = A \exp\left(-\frac{B}{T - T_0}\right) \tag{7}$$

with temperature-independent empirical parameters A, B and T_0 was fitted to the data in figures 3 and 4 and to similar data for the other f and d values in BR and in Gelsil. The values of the fitting parameters are given in table 1 (the measured values for CPG, the corrected ones for BR).

3.3. Shifts of glass transition temperature ΔT_g

A typical example of TSDC measurements is shown in figure 5: a TSDC thermogram in the temperature region of the peak due to the α process. We observe that the TSDC peak for the confined liquid is shifted to lower temperatures compared to the bulk liquid. We recall that TSDC thermograms are equivalent to ε'' thermograms at fixed frequencies in

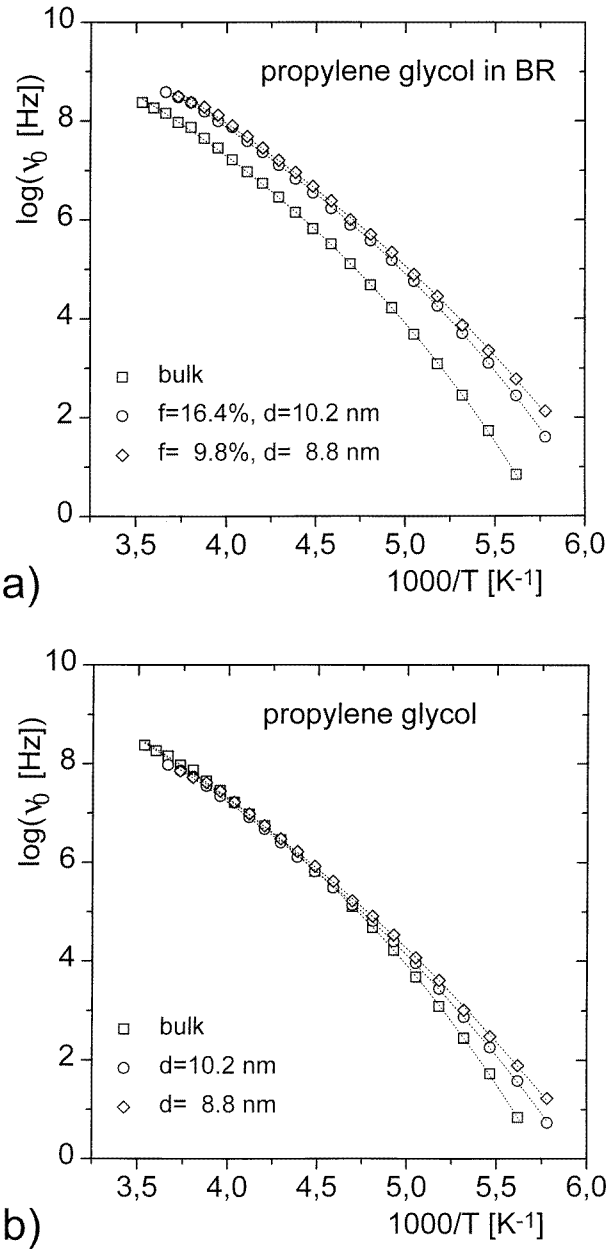

Figure 4. Arrhenius plot for the α process in PG bulk (□) and PG confined in BR with mean droplet diameter $d = 10.2$ nm (○) and 8.8 nm (◇), as measured (a) and corrected after Maxwell–Garnett theory, details in text (b). The lines are VFT (7) fits to the data.

the range 10^{-4}–10^{-2} Hz [24, 39]. T_m is in the temperature region of the calorimetric glass transitions and it changes with material and experimental conditions in the same sense as the calorimetric T_g [6, 24].

Table 1. Values of the empirical parameters $\log A$, B and T_0, as well as of the glass transition temperature T_g and of its shift $\Delta T_g = T_g(\text{bulk}) - T_g(\text{confined})$, obtained from the fits of the VFT equation (7) to the experimental data of DRS. For BR the values have been corrected after Maxwell–Garnett theory, details in text.

Matrix		d (nm)	$\log A$	B (K)	T_0 (K)	T_g (K)	ΔT_g (K)
Bulk			13.3	840.8	110.7	162.8	
Vycor		4.0	14.5	1157.0	80.5	147.5	15.3
Gelsil		2.5	14.5	1059.5	89.4	150.7	12.1
Gelsil		5.0	13.7	959.3	94.6	152.6	10.2
Gelsil		7.5	14.0	971.0	100.5	158.5	4.3
BR	$f = 7.1$	8.2	14.6	1178.1	83.9	151.6	11.2
BR	9.5	8.8	14.1	1127.3	86.0	152.5	10.3
BR	12.5	9.4	14.2	1075.7	94.0	157.4	5.4
BR	14.0	9.6	13.7	977.6	96.5	155.9	6.9
BR	16.4	10.2	13.6	977.3	96.8	156.4	6.4

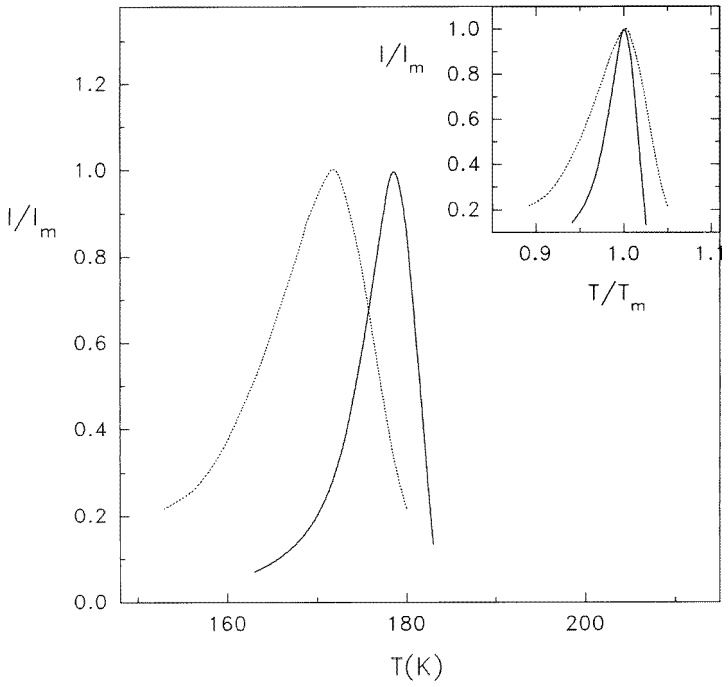

Figure 5. TSDC plots, normalized to unit height, of the α process of PG bulk (——) and confined in BR (– – –) (filling factor $f = 16.4\%$, mean droplet diameter $d = 10.2$ nm). The inset shows the corresponding scaling plot, I/I_m against T/T_m.

A detailed comparison of dielectric and calorimetric data on several glass-forming liquids and polymers shows that the temperature T_g^{diel} at which the dielectric relaxation time τ becomes 100 s (i.e. $\nu_0 = 1/628$ s^{-1}) is a good measure of the calorimetric glass transition temperature T_g [6, 18–21]. This point will be discussed in more detail in the next section. T_g^{diel} was obtained from extrapolation of the data similar to those shown in figures 3 and 4 to lower frequencies/temperatures. In the case of BR the corrected ΔT_g

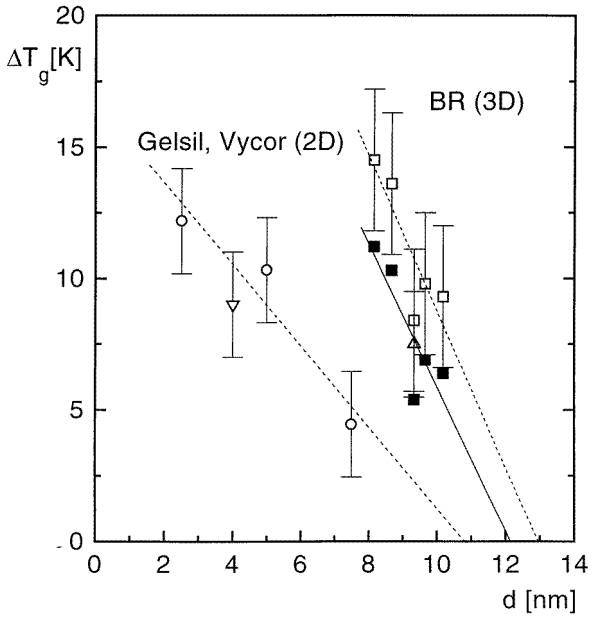

Figure 6. Glass transition temperature depression, $\Delta T_g = T_g(\text{bulk}) - T_g(\text{confined})$, against size of confinement (nomimal pore/droplet diameter d) for PG in BR with (■) and without correction after Maxwell–Garnett theory (□) and in Gelsil (○). △ and ▽ denote TSDC data for PG in BR and in Vycor glass, respectively. Vertical bars indicate experimental errors. The lines are to guide the eyes.

values are smaller than the uncorrected ones by about 3 K (figure 6); those for CPG are expected to be smaller. In what follows the unique term T_g will be used for both T_g^{diel} and T_g^{TSDC}. In any case, the quantity of interest is not T_g itself (absolute value), but the shift $\Delta T_g = T_g(\text{bulk}) - T_g(\text{confined})$.

Table 1 lists T_g and ΔT_g values determined from DRS data following the procedure described above. Figure 6 shows ΔT_g against pore/droplet diameter for PG confined in BR and in CPG. For BR both the corrected and the uncorrected ΔT_g values are shown. For comparison TSDC data obtained with PG in Vycor glass ($d = 4.0$ nm) and in BR ($d = 9.4$ nm) are also shown. In all systems studied T_g is lower in the confined liquid compared to bulk. For the same system ΔT_g decreases with increasing d. The effects are stronger in BR than in CPG.

3.4. The shape of the α process

In the following we consider the effects of confinement on the width and the shape of the response. Figure 7 shows a log–log scaling (master) plot of the normalized dielectric loss against reduced frequency for PG bulk and PG confined in Vycor glass at the same temperature together with the HN (2) fits. We observe that the loss peak becomes broader for the confined liquid. Similar broadening of the response was observed with Gelsil and with BR. In agreement with that, the TSDC peaks are broader for the confined liquid (figure 5, $\Delta T = 4.5$ K for PG bulk and 7.5 K for PG in Vycor glass, where $\Delta T = T_m - T_1$, T_m is the TSDC peak temperature and T_1 the temperature at which the current drops to half its maximum value on the low-temperature side of the peak).

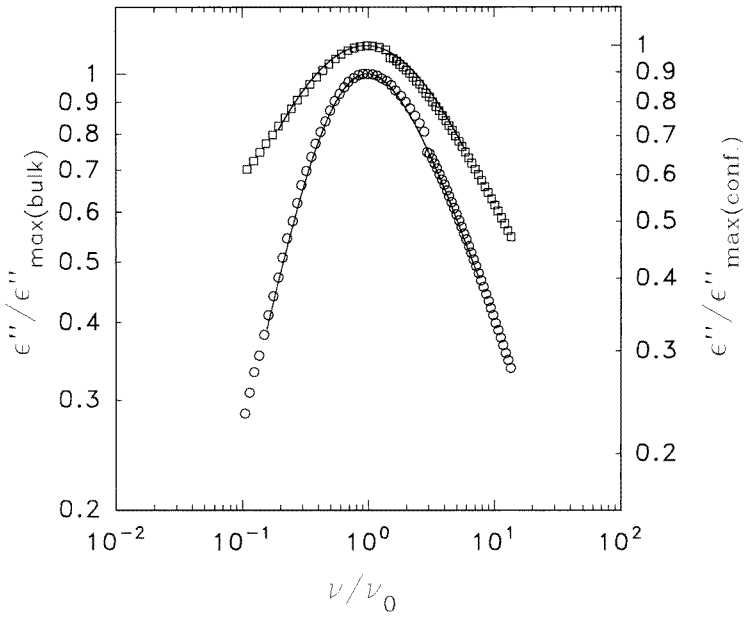

Figure 7. Log–log scaling plot of the normalized dielectric loss against reduced frequency for PG bulk (○) and PG confined in Vycor glass (□) at 210 K. The lines are HN fits (2) to the data.

It is well established that in bulk glass-forming liquids the dielectric a loss peak becomes broader with the temperature decreasing towards T_g and that this broadening is asymmetric, occuring predominantly on the high-frequency side of the peak [42]. Our results in figure 8(a) obtained with bulk PG confirm this behaviour. In contrast, the results in figure 8(b) obtained with PG confined in Vycor glass show that with T decreasing towards T_g significant broadening occurs on the low-frequency side of the peak and that the response becomes more symmetric compared to bulk.

The results concerning the shape of the response will be rationalized by means of the HN expression (2). The shape of the dielectric loss function near a loss peak is characterized by two shape parameters m and n ($0 \leqslant m$, $n \leqslant 1$) related to the limiting behaviour of the relaxation function [41, 43].

$$\begin{aligned} &\varepsilon''(\nu) \sim \nu^{m} \qquad (\nu \ll \nu_0) \\ &\varepsilon''(\nu) \sim \nu^{-n} \qquad (\nu \gg \nu_0). \end{aligned} \tag{8}$$

The HN parameters α and γ in equation (2) are related to the shape parameters by $m = 1-\alpha$ and $n = (1-\alpha)\gamma$. Thus, m and n can be obtained by fitting the HN expression to the experimental data and the results can be discussed in terms of models proposed for the interpretation of m and n and for the prediction of the relaxational behaviour of materials [43, 44].

Figure 9 shows the shape parameters m and n for PG bulk and PG in BR with $f = 16.4\%$ and $d = 10.2$ nm as a function of normalized reciprocal temperature, T_g/T. For bulk PG $m = 1$ and n increases with increasing temperature. For PG in BR n, $m < 1$, $n \neq m$ (asymmetric shape) and n is practically independent of T. The results in figure 9 are representative for BR at different filling factors f, the values of m and n becoming slightly smaller with decreasing filling factor f and mean droplet diameter d.

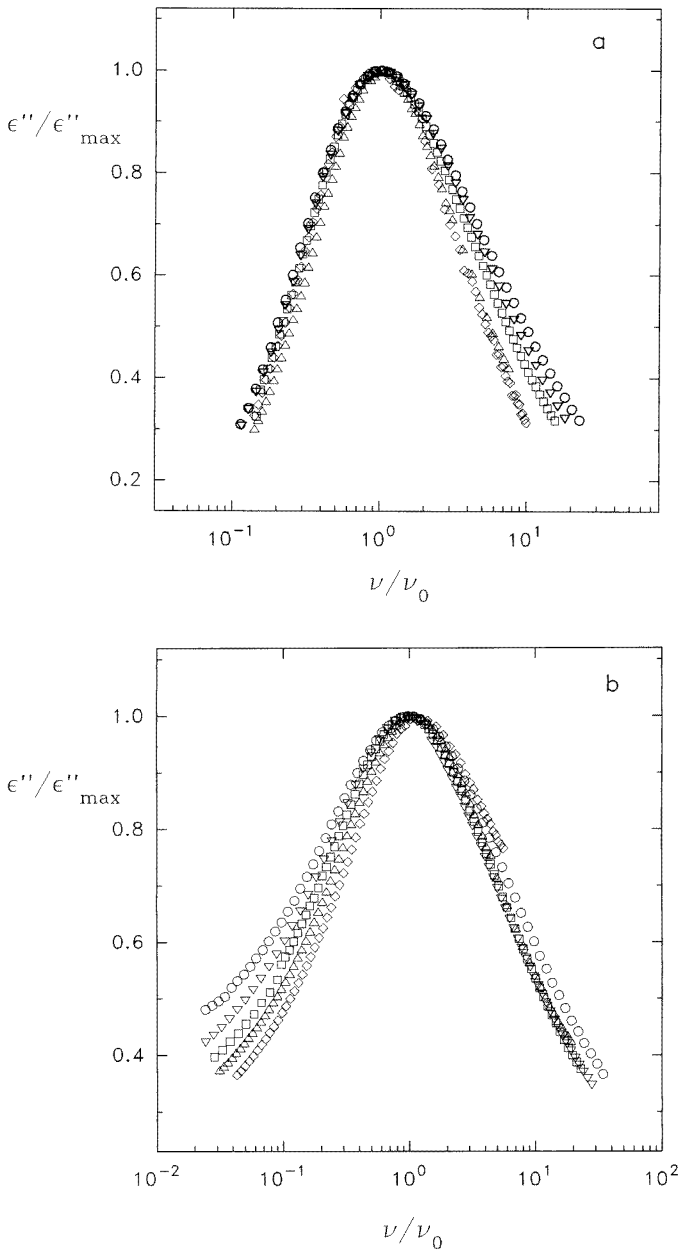

Figure 8. Scaling plots of the normalized dielectric loss against reduced frequency for PG bulk (a) and PG confined in Vycor glass (b) at several temperatures: 180 K (○), 200 K (▽), 230 K (□), 250 K (△) and 270 K (◇).

Figure 10 shows m and n for PG in Gelsil with $d = 5.0$ and 7.5 nm. Similar to PG in BR, m and n are smaller than in bulk and decrease with decreasing d. The main difference from BR is that here the response becomes symmetric, $\gamma \approx 1$ in the HN function and $m \approx n$. In figure 11 we show the results for PG in Vycor glass ($d = 4.0$ nm). Both m and n are

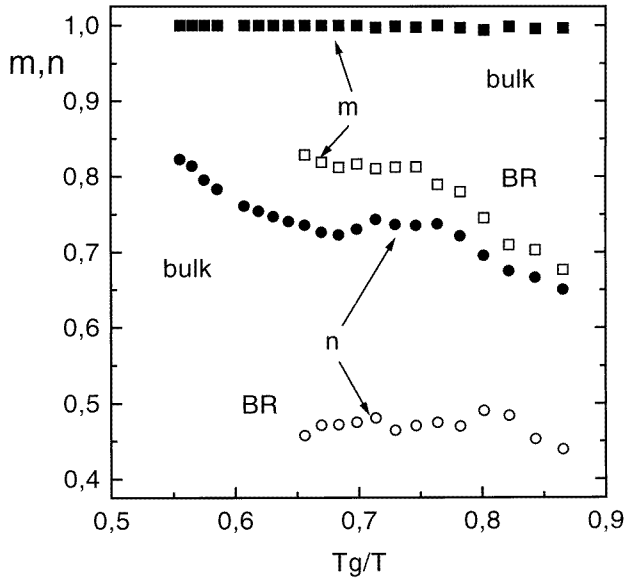

Figure 9. Shape parameters m and n for the α process of PG bulk (filled symbols) and PG in BR (open symbols, filling factor $f = 16.4\%$, mean droplet diameter $d = 10.2$ nm) against scaled reciprocal temperature, T_g/T.

smaller for the confined liquid compared to bulk and decrease with decreasing temperature. The main result concerns the degree of asymmetry of the response: the response becomes more symmetric compared to bulk.

A comment on the accuracy in the determination of the shape parameters m and n (and of the relaxation strength $\Delta\varepsilon$) from HN fits (2) and (8) is here in order. The use of two shape parameters increases the ambiguity of the fitting procedure, in particular in the case of overlapping of the loss peak under consideration with other peaks (which is however not strong for the α loss peak in our measurements). As a result, several sets of fitting parameters may give practically equally good fits. However, the changes of the shape parameters in figures 9–11 induced by confinement are larger than any uncertainty in their determination.

4. Discussion

4.1. The overall dielectric response

Our results show that the effects of confinement are different for the same liquid in different confining geometries justifying the methodology followed in this work. Several controlled porous glasses (CPGs) have been used in previous investigations [6, 14, 15, 18–22], including Vycor glass [6] and Gelsil glasses [20–22]. In these glasses the pores form a network and confinement of the liquid in the pores is two dimensional (2D). In butyl rubber (BR), in contrast, the liquid is confined in droplets i.e. confinement is 3D, with diameters in the range of a few nm, as revealed by SAXS measurements [37], in agreement with similar measurements on water confined in the same BR samples [23]. With respect to the dimensionality of confinement, it is interesting to note that microemulsions, used by MacFarlane and Angell [16] to confine glass-forming liquids and to investigate their glass

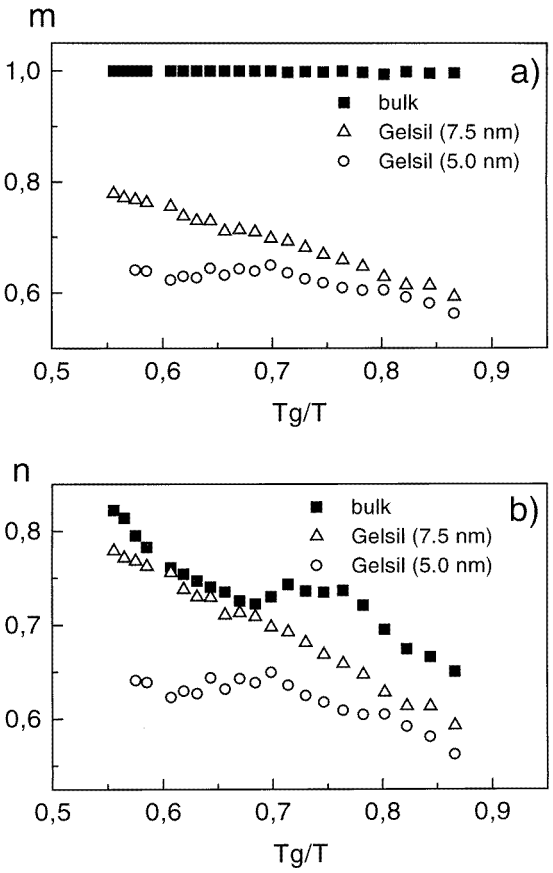

Figure 10. Shape parameters m (a) and n (b) for the α process of PG bulk (■) and PG confined in Gelsil glasses with mean pore diameter 7.5 nm (△) and 5.0 nm (○) against T_g/T.

transition properties by DSC, present also a system of 3D confinement. In the following we discuss the results of our investigation bearing in mind the difference in the dimensionality of confinement in BR and in CPG. These results are discussed also in relation to those of similar studies on polymers confined in thin films (1D confinement) [11, 13, 28–32], and in semicrystalline samples [33, 34] and on confined liquid crystals [8, 35, 36].

The CPGs and the BR used in this work were dielectrically neutral, in the sense that, in the temperature and frequency range of our measurements, the dielectric losses ε'' of empty samples are negligible compared to those of liquid-filled samples. BR exhibits a glass transition itself at temperatures around 200 K [23], with negligible dielectric loss however.

A significant advantage of BR compared to CPG is that dc conductivity effects in the liquid-filled samples are significantly weaker for BR (figure 1). A plausible explanation of this behaviour is that it is due to the fact that in BR the liquid is confined in droplets dispersed in the matrix and isolated from each other, whereas in CPG the liquid is confined in interconnected pores which form a continuous network. Because of the weaker conductivity effects in BR at low frequencies, as compared to CPG (figure 1), the analysis of the low-frequency response into two relaxations, Rel I and Rel II (figure 2) is more straightforward and unambiguous in BR than in CPG.

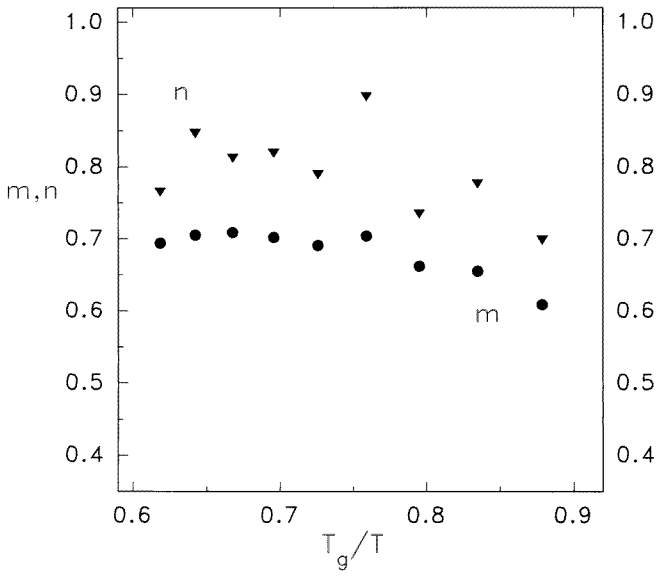

Figure 11. Shape parameters m (●) and n (▼) for the α process of PG confined in Vycor glass ($d = 4.0$ nm) against T_g/T.

Rel I and Rel II in figure 2 have been assigned to a slow liquid surface layer and to interfacial Maxwell–Wagner–Sillars polarization, respectively, for reasons discussed in the previous section and in agreement with previous work [18–20]. (This assignment is in disagreement with [21] where Rel I was assigned to Maxwell–Wagner polarization and Rel II to an interfacial layer.) An important implication of this assignment is that, in a sense, surface (chemical) effects are separated from confinement (physical) effects [4, 10–13]: surface interactions cause a fraction of the confined liquid in close contact to the walls to become relatively immobile (Rel I, interfacial layer), whereas the central fraction of the liquid (in the centre of the pores/droplets) experiences only confinement effects (α process). This separation of physical and chemical effects, as a result of the broad frequency range covered and of the sensitivity of DRS, might be a significant advantage of DRS compared to other techniques for confinement investigations.

The interpretation of our data is based on a two-state model, as a direct consequence of the results shown in figure 1: a relatively immobile surface part and a volume part, which experiences pure confinement effects [19]. A two-state model with dynamic exchange between a bulklike phase in the pore volume and an interfacial phase close to the pore wall has also been used to explain the results of DRS measurements on glass-forming liquids confined in Gelsil glasses [21]. (The two-state model is here used in a qualitative way and the question as to whether dynamic exchange has to be taken into account is therefore not discussed.) An alternative interpretation in terms of a mesoscopically uniform but cooperative relaxation as stimulated by the theoretical work of Sappelt and Jäckle [4] has also been proposed [45]. In a recent paper Jérôme and Commandeur combine both pure confinement and substrate effects in a picture of a uniform collective relaxation to interpret the results of second-harmonic generation measurements on the relaxation behaviour of molecules of a glass-forming liquid crystal confined in a thin film on a silica plate [8].

A direct consequence of the two-state model is that the α process studied in detail in our work refers to the inner mobile layer only and not to the whole mass of confined liquid, i.e. to dimensions smaller than the nominal diameter of the pores. This has important implications, e.g. if these and similar data are used to estimate the cooperativity length ξ.

Figure 12 shows the normalized amplitude I_n of the TSDC peak (normalized to the same polarizing field and heating rate [24, 39]) of the α process of PG in BR against filling factor f. I_n is a measure of the contribution of a TSDC peak to the static permittivity [24, 39], i.e. a measure of the relaxation strength $\Delta\varepsilon$. We observe in figure 12 that I_n increases overlinearly with increasing f. We recall that the mean droplet diameter d increases with increasing f. This behaviour can be understood in terms of the two-state model (and, thus, provides support for that model): with increasing f and d the relative amount of liquid in the immobile interfacial layer, which does not contribute to the α process, decreases with the result that $\Delta\varepsilon$ and I_n increase overlinearly.

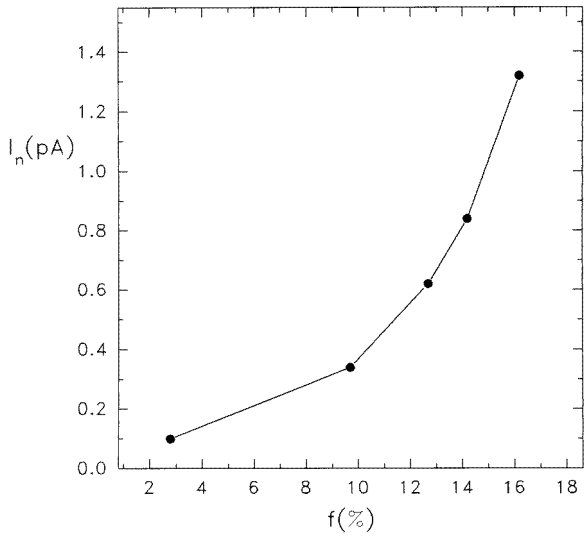

Figure 12. Normalized amplitude I_n of the TSDC peak of the α process of PG in BR against filling factor f. The lines are to guide the eyes.

4.2. Arrhenius plots and relaxation times

The Arrhenius plots in figures 3 and 4 and the TSDC plots in figure 5 show that the dynamics of the α process becomes faster in the confined liquid. For the same system the effects become stronger with decreasing confining length d and, for the same d, with decreasing temperature. They are stronger in BR than in CPG (3D versus 2D confinement).

These results can be understood on the basis of the cooperativity in the configurational entropy model of glass formation of Adam and Gibbs [9], see also section 1. This model explains the temperature dependence of relaxation phenomena in glass-forming liquids essentially in terms of the temperature dependence of the size of the cooperatively rearranging region. The size ξ of this region is shown to be determined by its content of configurational entropy. The relaxation time τ of the cooperatively rearranging region increases with increasing ξ. If, at a given temperature, the size of the confined sample

L (thickness of the inner mobile layer/sphere in our experiments) is less than ξ, all the molecules in the sample will take part in the cooperative dynamics and, as a result, the sample will relax faster than the bulk sample. This effect will become stronger with decreasing sample size. If, on the other hand, the size of the confined sample is larger than ξ, there is no size dependence in the dynamical behaviour. Further ξ decreases with increasing temperature [3, 4], so that for a given sample size L confinement effects become weaker with increasing temperature and finally disappear (figure 4(b)). For quantitative estimations it should be taken into account that the real sample size L (i.e. the size of the mobile inner layer) increases with increasing temperature towards the nominal confining length d [10, 21, 22]. These relations are schematically illustrated in figure 13.

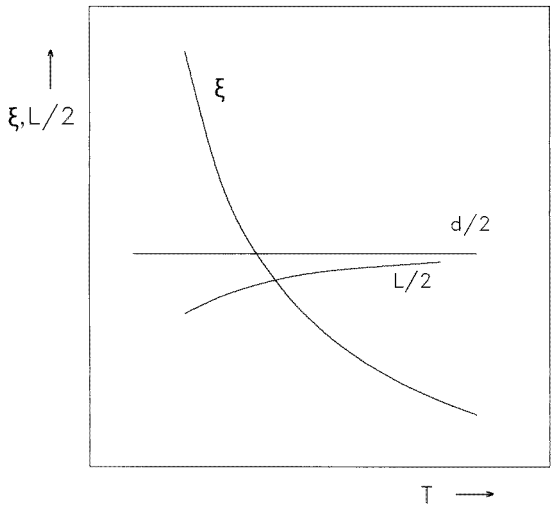

Figure 13. Schematic diagram of cooperativity length ξ, confining length d and real sample size L against temperature T. Confinement effects occur for $L < \xi$ and increase in intensity with increasing difference $\xi - L$. For $L > \xi$ no confinement effects occur.

Using kinetic Ising and lattice-gas models with kinetic constraints as models of cooperative dynamics in undercooled liquids near the glass transition Sappelt and Jäckle concluded that confinement of glass-forming liquids in geometries of confining length comparable to the cooperativity length ξ should lead to retardation of the α process and to an increase of the glass transition temperature T_g [4]. The reason for that is that with the confining length decreasing below ξ, an increasing number of molecules are permanently blocked and no longer contribute to the response of the system to external perturbations [4]. Monte Carlo simulations by Ray and Binder [7] of the dynamics near the glass transition in a two-dimensional lattice model of polymer melt, on the other hand, show that, at low temperature, the diffusion constant increases with decreasing size of the sample. According to the authors, these results suggest the possibility of the existence of cooperatively rearranging regions [9], whose mean size increase as the temperature is lowered.

The results in figures 3 and 4 suggest that the confinement effects become weaker with increasing temperature and finally disappear (figure 4(b) with corrected relaxation rates), as a result of the decrease of ξ with increasing temperature (figure 13). Thus, the crossover temperature can be interpreted as the temperature where the onset of the cooperativity

of the molecular motion takes place [7]. In fact dielectric measurements in glass-forming liquids in bulk indicate the existence of a crossover temperature separating local (Arrhenius temperature dependence) and cooperative motional process (Vogel–Fulcher–Tamman temperature dependence) [46]. The transition was found to be more pronounced for non-associating compared to H-bonded liquids, a prediction which would be interesting to check for confined liquids also. Systematic studies on glass-forming liquids and the use of new temperature derivative methods of evaluation of the experimental data have indicated an additional crossover to a further VFT dependence at lower frequencies (temperatures) [47, 48]. The frequency range of our measurements should be extended in further studies to lower frequencies to check for possible analogous effects in confined liquids.

4.3. Shifts of glass transition temperature ΔT_g

We discuss now the shift of the glass transition temperature T_g, $\Delta T_g = T_g(\text{bulk}) - T_g(\text{confined})$ (figure 6). T_g was determined by means of DRS by the condition $\tau(T_g) = 100$ s, where τ is the dielectric relaxation time of the α process, $\tau = 1/2\pi\nu_0$ [6, 18–21], and by means of TSDC as the peak temperature of the α process (figure 5) [6]. DRS and ac DSC measurements on salol (phenyl salicylate) have shown that the corresponding Arrhenius plots practically coincide in the common frequency range of the two techniques [49], which suggests that both techniques probe at glass transition the mobility of units of similar size. This justifies best the use of dielectric techniques to measure glass transition temperatures.

ΔT_g in figure 6 decreases with increasing pore (droplet) diameter. ΔT_g values corrected after Maxwell–Garnett (section 3.2) are about 3 K smaller than uncorrected values (figure 6). The corrections are expected to be smaller for CPG. In general, similar ΔT_g values are obtained from DRS and TSDC, as revealed by measurements on other liquids too (work in progress). These measurements confirm also another result shown in figure 6, namely that similar ΔT_g values are measured for both CPGs used, Vycor glass and Gelsil. For similar d values ΔT_g values are significantly larger for BR than for CPG. Bearing in mind that the α process in the confined systems reflects the properties of the inner mobile layer only (pure confinement effects) we conclude that ΔT_g are significantly larger for three-dimensionally than for two-dimensionally confined PG.

Despite the very different values of ΔT_g for BR and CPG in figure 6, ΔT_g vanish for both systems at $d \approx 10$–12 nm. This allows us to determine the cooperativity length ξ as $\xi \leqslant 5$–6 nm (figure 13). Please note that the real sample size L is smaller than d due to the presence of the relatively immobile interfacial layer (figure 13); therefore 5–6 nm is an upper limit for ξ. Values of ξ at T_g for glass-forming liquids reported in the literature are a few nm: $\xi \leqslant 1$ nm for propylene glycol, butylene glycol and pentylene glycol [20], $\xi \leqslant 0.7$ nm for glycerol [21], $\xi \approx 3$ nm for 2-methyltetrahydrofuran [25], $\xi \geqslant 7$ nm for phenylsalicylate (salol) [50], $\xi \leqslant 10$–12 nm for N-methyl-ε-caprolactam (to be published). Obviously further work is needed to determine ξ more accurately and to check for possible systematic changes with the nature of the liquid (e.g. H-bonded versus non-associating liquids and fragility [51]).

The shift of T_g to lower temperatures in the confined liquid can be understood following our explanation for the acceleration of the α process: the relaxation becomes faster in the confined liquid so that T_g ($\tau(T_g) = 100$ s) shifts to lower temperatures. The shift increases with decreasing confining length d (and sample size L) (figure 13) and with increasing dimensionality of confinement. The lowering of T_g for the confined liquid is in agreement with theoretical predictions by Hunt [5] and in disagreement with the results of molecular

dynamics simulations for one-dimensionally confined liquid [12]. The explanation that the shift of T_g towards lower temperature in real liquids may be due to details of the interface [12] is in contradiction with the experimental results (this work, [14, 19]).

Positive shifts ΔT_g have been measured by DSC on several liquids confined in (both treated and native) CPG [14, 15]. We note here that the observed ΔT_g values were different for different liquids, decreased with increasing pore diameter d and were still present at relatively large values of d [14]. Practically no shifts were observed in liquids confined in microemulsions [16] and in hydrogels [17]. We speculate that this may be due to the relatively broad distribution of droplet sizes and the penetration of droplet by surfactant in the microemulsions [16] and to the rather irregular form of pores and voids in the hydrogels [17].

It is interesting to compare the results obtained with confined liquids with those obtained with confined polymers [11, 13, 28–34, 52, 53]. Several experimental techniques have been used to measured more or less directly T_g in thin polymeric films (1D confinement), typically supported on a substrate. Depending on film thickness, polymer and substrate, shifts of T_g to both lower [11, 28, 30, 32] and higher [11, 13] temperatures, compared to bulk, have been measured. Although often a two-layer model (in [30] a three-layer model, incorporating a dead layer near the substrate, a surface layer with reduced T_g and a bulklike layer between these interfaces) has been used to explain the results, it is not always clear to which layer the measured T_g refers. It has also been suggested that a region with an elevated T_g exists near the polymer–substrate interface [53]. Measurements on free standing polystyrene films, on the other hand, show that, compared to bulk, T_g decreases linearly with decreasing film thickness [29]. Schick and Donth [33] and Laredo *et al* [34] measured the glass transition properties of specially prepared semicrystalline polymer samples in the hope of detecting confinement effects on the amorphous phase. The advantage of semicrystalline polymers for such studies is that the same material is used for confinement (no chemical effects), the disadvantage being that the constraints imposed upon the amorphous regions by the crystalline regions may dominate over the pure confinement effects. Whereas no shift of T_g was observed in polyethylene terephthalate, where the amorphous phase forms films [33] (1D confinement), a shift of T_g to lower temperatures, compared to bulk, was observed in polycarbonate and related to speculations on the organization of the mobile amorphous phase in droplets [34] (3D confinement). Finally, DSC measurements on polystyrene microparticles, prepared by freeze-drying a very dilute cyclohexane solution and by spraying a dilute benzene solution into methanol, showed a significant lowering of T_g compared to bulk [52].

Interesting effects of confinement were observed on the collective dynamics of the isotropic–nematic phase transition of liquid crystals confined in CPG [35, 36]. The transition shifts to lower temperatures, the transition region becomes broader and the bulk nematic phase is replaced by a 'glassy' state [35]. Measurements in the bulk pretransitional region show a drastic decrease of the relaxation time compared to the bulk [36].

4.4. The shape of the α process

In the following we discuss the effects of confinement on the width and the shape of the response (figures 7–11). Both the DRS (figure 7) and the TSDC response (figure 5) are broader for the confined liquid compared to the bulk, in agreement with the results of measurements on confined liquids [6, 14–21], confined polymers [31] and confined liquid crystals [35, 36]. The broadening of the dielectric response of the confined liquid may be linked to increased local scale heterogeneity [31], in analogy to the broadening of

the α relaxation distribution in bulk glass-forming liquids and polymers as temperature is decreased towards T_g (figure 8) having been linked to increased heterogeneity caused by local density fluctuations [54].

In this work the shape of the response has been described by the two shape parameters m, n (equations (8)). For the discussion we refer to two models proposed for the interpretation of m and n and for the prediction of the relaxational behaviour of materials [43, 44]. In the cluster model of Dissado and Hill (DH model) [43] n describes the interactions within the cluster (region of cooperative interactions) and m the cluster–cluster interactions. n decreases with increasing correlation of the motions within the cluster, whereas m increases with increasing correlation of the long-range motions. In the model of Schönhals and Schlosser (SS model) for polymers at the glass transition [44] n describes the local chain motions and decreases with increasing hindrance of these motions. m is related to the large-scale motions and decreases with increasing long-range correlation.

In bulk PG $m = 1$ over the whole temperature range and $n < 1$ increasing with increasing temperature (figure 9), in quantitative agreement with Schönhals *et al* [42]. In PG confined in BR both m and n are smaller than 1; m increases with increasing temperature, whereas n is practically constant around 0.45 (figure 9), i.e. n takes values lower than 0.5 [42]. With respect to the aforementioned models, it follows that, in terms of both models, confinement results in an increase of the correlation of short-range (local) motions (n decreases). The lowering of m by confinement implies an increase (SS model) or a decrease (DH model) of the correlation of long-range motions. Further, confinement to dimensions less than the cooperativity length ξ should result in a suppression of the correlation of long-range motions, so that our results are in favour of the DH rather than the SS model.

The discussion in the previous paragraph of the changes in m and n induced by confinement is in the main points valid also for PG in Gelsil (figure 10) and in Vycor glass (figures 8 and 11). The main difference from BR is that the shape of the response, which is asymmetric for PG bulk and PG in BR, becomes more symmetric in Vycor glass and symmetric ($m \approx n$) in Gelsil. The broadening of the response induced by confinement is more asymmetric than in the case of BR, occurring predominantly on the low-frequency side (figure 7), i.e. affecting more m than n (figure 10). In this respect the behaviour of the liquid in the CPG resembles that of semicrystalline polymers [55]. We can only speculate at this stage that the similarity may arise from similar constraints upon the amorphous phase imposed by the crystallites in the semicrystalline samples and the rigid porous matrix in the CPG. We note also that the values of m are rather similar to each other in BR and CPG, whereas those of n are clearly lower in BR than in CPG. Within both the DH and the SS models this implies increased correlation of short-range (local) motions in BR compared to CPG, which might be linked to the dimensionality of confinement. Measurements in progress on non-associating liquids should help to further clarify these points.

5. Conclusions

We presented the results of a detailed investigation of the effects of confinement on the dynamics of the glass transition in the glass-forming liquid propylene glycol. We took advantage of the ability of measuring the same liquid in different three- and two-dimensionally confined geometries and of the broad frequency range and of the high sensitivity and resolving power, respectively, of the DRS and the TSDC techniques used for the investigation. In the case of BR, relaxation rates and glass transition temperatures determined by DRS have been corrected after Maxwell–Garnett theory [25–27]. The

corrections in T_g values are small; even smaller corrections are expected for CPG. Our conclusions can be summarized as follows.

(1) Liquid–wall interactions give rise to a slow relaxation process of a relatively immobile interfacial layer (corresponding to a higher glass transition temperature compared to the bulk liquid), whereas the volume liquid experiences pure confinement effects (two-state model).

(2) The α relaxation associated with the glass transition is faster for the confined volume liquid compared to the bulk liquid. This effect becomes stronger with decreasing confining length d and with decreasing temperature towards the glass transition temperature T_g.

(3) As a result of the acceleration of the α relaxation, T_g is lower for the confined volume liquid compared to the bulk liquid. $\Delta T_g = T_g(\text{bulk}) - T_g(\text{confined})$ decreases with increasing d, becoming zero for $d \approx 10$–12 nm, and is larger for the three-dimensionally confined liquid compared to the two-dimensionally confined one.

(4) The acceleration of the α relaxation and the lowering of T_g can be understood on the basis of the cooperativity concept and the configurational entropy model of Adam and Gibbs.

(5) The cooperativity length or characteristic length of the glass transition ξ is determined for both butyl rubber and controlled porous glasses used in this work to $\xi \leqslant 5$–6 nm at T_g.

(6) The α relaxation becomes broader for the confined volume liquid compared to the bulk liquid, the broadening being larger in the case of 3D confinement. The shape of the response is described by two shape parameters and is discussed in terms of the Dissado–Hill and of the Schönhals–Schlosser model, being in favour of the first one.

Propylene glycol, studied in detail in this paper, is a typical H-bonded liquid. Work on N-methyl-ε-caprolactam, as a representative of non-associating glass-forming low molecular weight liquids, in the same confining geometries, is in progress and the results will be published in a future paper. Measurements on other monomeric and oligomeric liquids, studied in detail in the bulk to elucidate special aspects of the glass transition, e.g. selected on the basis of the fragility scheme [51], may contribute to a better understanding of the phenomenon of glass transition.

References

[1] Jäckle J 1986 *Rep. Prog. Phys.* **49** 171
[2] Götze W 1991 *Liquids, Freezing and the Glass Transition* ed J P Hansen, D Levesque and J Zinn-Justin (Amsterdam: North-Holland) p 291
[3] Donth E 1992 *Relaxation and Thermodynamics in Polymers, Glass Transition* (Berlin: Akademie)
[4] Sappelt D and Jäckle J 1993 *J. Phys. A: Math. Gen.* **26** 7325
[5] Hunt A 1994 *Solid State Commun.* **90** 527
[6] Pissis P, Daoukaki-Diamanti D, Apekis L and Christodoulides C 1994 *J. Phys.: Condens. Matter* **6** L325
[7] Ray P and Binder K 1994 *Europhys. Lett.* **27** 53
[8] Jérôme B and Commandeur J 1997 *Nature* **386** 589
[9] Adam G and Gibbs J H 1965 *J. Chem. Phys.* **43** 139
[10] Drake J M and Klafter J 1990 *Phys. Today* **43** 46
[11] Keddie J L, Jones R A L and Gory R A 1994 *Faraday Discuss.* **98** 219
Keddie J L, Jones R A L and Gory R A 1994 *Europhys. Lett.* **27** 59
[12] Fehr T and Löwen H 1995 *Phys. Rev.* E **52** 4016
[13] van Zanten J H, Wallace W E and Wu W-L 1996 *Phys. Rev.* E **53** R2053
[14] Jackson C L and McKenna G B 1991 *J. Non-Cryst. Solids* **131–133** 221
[15] Zhang J, Liu G and Jonas J 1992 *J. Phys. Chem.* **96** 3478
[16] MacFarlane D R and Angell C A 1982 *J. Phys. Chem.* **86** 1927
[17] Hofer K, Mayer E and Johari G P 1991 *J. Phys. Chem.* **95** 7100

[18] Schüller J, Mel'nichenko Yu B, Richert R and Fischer E W 1994 *Phys. Rev. Lett.* **73** 2224
[19] Schüller J, Richert R and Fischer E W 1995 *Phys. Rev.* B **52** 15 232
[20] Gorbatschow W, Arndt M, Stannarius R and Kremer F 1996 *Europhys. Lett.* **35** 719
[21] Arndt M, Stannarius R, Gorbatschow W and Kremer F 1996 *Phys. Rev.* E **54** 5377
[22] Streck C, Mel'nichencko Yu B and Richert R 1996 *Phys. Rev.* B **53** 5341
[23] Pelster R, Kops A, Nimtz G, Enders A, Kietzmann H, Pissis P, Kyritsis A and Woermann D 1993 *Ber. Bunsenges. Phys. Chem.* **97** 666
[24] van Turnhout J 1980 *Electrets* ed G M Sessler (Berlin: Springer) p 81
[25] Yan Y, Streck C and Richert R 1997 *Mat. Res. Soc. Symp. Proc.* vol 464 (Pittsburgh, PA: Materials Research Society) p 32
[26] van Beek L K H 1967 *Progress in Dielectrics* vol 7, ed J B Birks (London: Heywood) p 69
[27] Dukhin S S 1971 *Surface and Colloid Science* vol 3, ed E Matijevic (New York: Interscience) p 83
[28] Reiter G 1993 *Europhys. Lett.* **23** 579
[29] Forrest J A, Dalnoki-Veress K, Stevens J R and Dutcher J R 1996 *Phys. Rev. Lett.* **77** 2002
[30] DeMaggio G B, Frieze W E and Gidley D W 1997 *Phys. Rev. Lett.* **78** 1524
[31] Hall D B, Hooker J C and Torkelson J M 1997 *Macromolecules* **30** 667
[32] Brucker O, Christian S, Bock H, Frank C W and Knoll W 1997 *ACS–Polym. Preprints* **88** 918
[33] Schick C and Donth E J 1991 *Phys. Scr.* **43**
[34] Laredo E, Grimau M, Müller A, Bello A and Suarez N 1996 *J. Polym. Sci. Polym. Phys.* **34** 2863
[35] Wu X I, Goldburg W I, Liu M X and Xue J Z 1992 *Phys. Rev. Lett.* **69** 470
[36] Schwalb G and Deeg F W 1995 *Phys. Rev. Lett.* **74** 1383
[37] Barut G 1996 *PhD Thesis* University of Cologne
[38] Pelster R 1995 *IEEE Microwave Theory Technol. Trans.* **MTT-43** 1494
[39] Pissis P, Ananagnstopoulou-Konsta A, Apekis L, Daoukaki-Diamanti D and Christodoulides C 1991 *J. Non-Cryst. Solids* **131–133** 1174
[40] Böttcher C J F and Bordewijk P 1978 *Theory of Electric Polarization* 2nd edn, vol 2 (Amsterdam: Elsevier)
[41] Jonscher A K 1983 *Dielectric Relaxation in Solids* (London: Chelsea Dielectrics)
[42] Schönhals A, Kremer F and Schlosser E 1991 *Phys. Rev. Lett.* **67** 999
[43] Dissado L A and Hill R M 1983 *Proc. R. Soc.* A **390** 131
[44] Schönhals A and Schlosser E 1989 *Colloid Polym. Sci.* **267** 125
[45] Richert R 1996 *Phys. Rev.* B **54** 15 762
[46] Schönhals A, Kremer F, Hofmann A, Fisher E W and Schlosser E 1993 *Phys. Rev. Lett.* **70** 3459
[47] Stickel F, Fischer E W and Richert R 1995 *J. Chem. Phys.* **102** 6251
[48] Stickel F, Fischer E W and Richert R 1996 *J. Chem. Phys.* **104** 2043
[49] Dixon P K 1990 *Phys. Rev.* B **42** 8179
[50] Arndt M, Stannarius R., Groothues H, Hempel E and Kremer F 1997 *Phys. Rev. Lett.* **79** 2077
[51] Angell C A 1991 *J. Non-Cryst. Solids* **131–133** 13
[52] Ding J, Xue G, Dai Q and Cheng R 1993 *Polymer* **34** 3225
[53] Wu W-L, van Zanten J H and Orts W J 1995 *Macromolecules* **28** 771
[54] Ngai K L and Plazek D 1995 *J. Rubber Chem. Technol.* **68** 376
[55] Ishida Y, Yamafuji K, Ito H and Takayanagi M 1962 *Koll. Z. Z. Polyum.* **184** 97